COMPUTATIONAL MODELING OF EXPANDING PLASMA PLUMES IN SPACE USING A PIC-DSMC ALGORITHM

David Y. Oh* and Daniel E. Hastings†
Department of Aeronautics and Astronautics
Massachusetts Institute of Technology
Cambridge, MA

Abstract

A computational model of the plume of a Stationary Plasma Thruster (SPT) has been developed using a quasi-neutral Particle-in-Cell/Direct Simulation Monte Carlo (PIC-DSMC) method. This model is based on previous work showing that the plume consists of a quasi-neutral, unmagnetized plasma with collisionless electrons. A three-dimensional version of the model has been developed and validated against an axisymmetric version and experimental data.

The three-dimensional PIC-DSMC model has been used to simulate an SPT-100 thruster mounted on a typical communications satellite. In addition, a surface sputtering model has been developed to predict the impact of the plume on satellite surfaces. Results are presented for an SPT-100 mounted at different angles with respect to the solar array. The results show that the thruster's cant angle has a large impact on the rate of erosion and the area over which erosion occurs. Future work is planned to convert the PIC-DSMC model to support simulations on unstructured meshes and to improve the code source model.

---

*ScD, Space Systems/Loral
†Professor of Aeronautics and Astronautics

Nomenclature

T_e = Electron Temperature
$\bar{c}_e$ = Mean Electron Thermal Velocity
c_r = Relative Speed between Collision Partners
e = Elementary Charge = 1.6×10^{-19} C
k = Boltzmann's Constant = 1.38×10^{-23} J/K
n_e = Electron Number Density
n_o = Reference Charge Density (arbitrary)
n_{ref} = Reference Electron Number Density
z = Axial Distance from Anode Exit
Γ_i = Ion Flux
φ = Electrical Potential

Introduction

When compared to chemical propulsion systems, electric propulsion offers substantial fuel savings for stationkeeping applications. One system which has shown particular promise is the Stationary Plasma Thruster (SPT), also referred to as the Hall Thruster. This device has a near optimum specific impulse for north-south stationkeeping and is being actively marketed for use on Western satellites. However, although SPTs have an extensive Russia flight heritage, they have yet to fly on a Western satellite. Western designers have expressed concern that the plasma plume emitted by the SPT may erode and contaminate the surfaces of satellites and interfere with communications signals. These concerns must be addressed before SPTs can be used for commercial applications.

In order to study plume contamination issues, a substantial amount of experimental work has been conducted. Ion fluxes and distributions have been determined and plume-induced sputtering and contamination have been measured in several ground experiments.[1-4] However, relatively little effort has been made to model processes occurring in the SPT's plume region. Those models which do exist are relatively simple and are not well-suited to modeling complex satellite geometries.[5,6] More detailed models are needed to fully characterize the plume and to understand the relationship between existing experimental data and actual operating conditions.

This paper presents an advanced computational model of an expanding SPT plume and validation of the model. The model uses a combination of the Particle-in-Cell (PIC) and Direct Simulation Monte Carlo (DSMC) methods to simulate collisions in the plume and track the flow of ions and neutrals across the domain. The basic PIC-DSMC algorithm has been described in previous work.[7] Many improvements have been made to the model, including the use of double ions, the addition of surface sputtering, and the development of an improved source model. Axisymmetric and three-dimensional versions of the code have been developed and validated against experimental data, and the simulation has demonstrated the ability to model the plume on meter-length scales. The resulting model runs on a UNIX workstation and should be useful to designers interested in evaluating the impact of an SPT on realistic satellite configurations.

The axisymmetric plume model has been verified against a variety of experimental data.[8] Simulated ion current density measurements are shown to match experimental data to within a factor of two to three on meter-length scales. A surface erosion model has also been shown to agree well with experimental data, though the results depend heavily on the sputtering coefficient. This paper presents the three-dimensional extension and results which simulate conditions beyond those which can be studied in ground-based experiments. These results include three-dimensional simulations of a SPT thruster mounted on a communications satellite. The paper concentrates on modeling the SPT-100 because it is the most extensively studied of the Hall thrusters at this time. In principle, the model can be modified and applied to new Hall and anode layer (TAL) thrusters as data becomes available.

Section 2 summarizes the PIC-DSMC algorithm and describes aspects of the model which are unique to the three-dimensional geometry, while section 3 presents results from a fully three-dimensional simulation of an SPT-100 mounted on a communications satellite. Finally, section 4 presents the conclusions.

Theory and Computational Method

PIC-DSMC Model

The PIC-DSMC model used in this paper has been described in detail in previous work.[7] This section briefly summarizes the basic algorithm and describes aspects of the model specific to a three-dimensional geometry. In particular, it focuses on the boundary conditions used to simulate the surfaces of satellites and their interaction with the surface erosion model. Details of the underlying method, including the axisymmetric model, are given in a previously published paper.[8]

The SPT-100 has been studied extensively in ground tests, and many of its basic characteristics are well documented. Table 1 gives the parameters used to model the thruster in the PIC-DSMC plume model.

Inner Anode Diameter[1]	56 mm
Outer Anode Diameter[1]	100 mm
Cathode Orifice Diameter[2]	0.5 mm
Propellant	Xe
Propellant Flow Rate[2]	5.2 mg./sec.
Fraction of Propellant Directed to Cathode[2]	~10%
Electron Temperature[3] (Te)	2 eV
Axial Ion Velocity[1]	~17000 m/s
Fraction of Ions which are Double Ions[1]	~20%
Fraction of Propellant Ionized in Discharge Chamber[2]	> 95%

Table 1: SPT-100 Basic Characteristics

Xe propellant is ionized in the anode and emerges from the thruster in the form of neutrals, ions, and double ions. The following statements can be made about the plume region.[7]

- The Debye length is small, so the plume is quasi-neutral except near surfaces.
- The ions are unmagnetized.
- The electrons are unmagnetized when z > 25 cm.
- The electrons are collisionless.

Based on these observations, we have constructed a quasi-neutral PIC-DSMC simulation of a Hall Thruster plume. The PIC-DSMC method uses macroparticles to statistically model gases at a molecular level. The particle equations of motion are integrated using the leapfrog method, and the electric field is obtained from the electric potential, which is in turn obtained by inverting the Boltzmann relationship:

$$n_e = n_{ref} \exp(e\phi / kT_e)$$

This procedure is valid for isothermal, collisionless, and unmagnetized electrons moving at low drift velocities. A constant electron temperature of 2 eV is assumed in these simulations.

Collisional processes are modeled between move steps using the DSMC method. Table 2 shows the collision processes included in the present PIC-DSMC model.

CEX	Elastic
Xe-Xe^{+}	Xe-Xe
Xe-Xe^{++}	Xe-Xe^{+}
	Xe-Xe^{++}

Table 2: Collisions covered in the simulation

Collisions between charged particles are not included, because it is computationally impractical to simulate them at the present time.[8]

Particles are loaded into the simulation at each time step to simulate the flow from a Hall thruster. The ion and neutral distribution functions are determined from an empirical model of an SPT-100 containing no free parameters.[8] Approximately 10% of the propellant entering an SPT-100 is diverted to the cathode. This flow is assumed to consist entirely of neutrals and is treated differently in axisymmetric and three-dimensional domains. In a three-dimensional geometry, the flow emerges from a cathode orifice which is placed 7.5 cm above and 1.0 cm downstream of the center of the anode exit. Both cathode and anode neutrals are assumed to have a temperature of 1000 K, and the flow is choked at the cathode and anode exits, respectively.

The major motivation for developing a three-dimensional plume model is to simulate realistic spacecraft geometries. The three-dimensional PIC-DSMC model is built on an embedded Cartesian mesh. A simulated bus, yoke, and solar array are shown in Figure 1 on a 3.2 m x 4.4 m x 3.2 m computational domain, and an embedded grid is visible along the edge of the main bus. This grid is collocated with the thruster and is used to better resolve the core of the plume. The section of bus shown has dimensions of 1.1 m x 1 m x 2.6 m and represents a quarter of the spacecraft's main bus. A 1.9 meter yoke connects the bus to the end of a solar array. The array is 1.5 meters wide and continues off the top of the domain. Only the bottom 2.7 meters of the array is included in the simulation, since it is this area which should experience the most plume degradation.

Sputtering Model

One issue of particular interest to satellite designers is the interaction of the plume with surfaces of a spacecraft. In order to study surface interaction issues, a surface sputtering model has been developed and incorporated into the PIC-DSMC model. The model, described below, is based upon a relatively simple model used for axisymmetric geometries.[8]

The SPT plume's primary impact on surfaces is to cause sputter-induced erosion damage. Plume-induced deposition, however, is ignored in the 3D model. Deposition can be safely ignored when modeling thrusters with ceramic anodes. In these cases, the eroded material is likely to be benign. This is consistent with experimental results that report little or no deposition on witness plates, even when they are placed at high angles with respect to the centerline.[9] Deposition probably cannot be ignored with TAL thrusters, however, which have metal anodes. In three-dimensional geometries, any particle crossing an object boundary is removed or reflected as appropriate for that species. Ions are neutralized and removed from the simulation while neutrals are reflected back into the domain in a manner consistent with an ideal specular surface.

When creating an object, it is necessary to specify its potential with respect to the plasma. A solar panel would be represented by an object of fixed potential. Different points on the array would be assigned different potentials to mimic the distribution of cells across the array. A thermal blanket or other electrically isolated object would be represented by surfaces with floating potentials. These objects would be treated as dielectrics whose potential is determined by balancing the flux of ions and electrons to the surface.

When a plasma interacts with an object, a sheath typically forms near exposed surfaces. Because no information passes from the sheath back into the pre-sheath region, it is possible to simulate flow up to the pre-sheath boundary without simulating the detailed structure of the sheath itself. The detailed structure of the sheath and the wall potential have no effect on the overall structure of the plume.

For surfaces of fixed potential, the boundary conditions are potentially more complex. When the surface potential is less than the local plasma potential, Numerical tests were applied to the three-dimensional model; the model was shown to conserve total energy, and the results were insensitive to the number of iterations and the number of particles in the simulation.

Figure 2 shows several plots of the ion current density 60 cm from the thruster exit at a pressure of 2.2 x 10^{-6} Torr. Three types of results are overlaid on the graph: an axisymmetric simulation (marked as "2D"), a three-dimensional simulation, and experimental data from Manzella.[3] The simulated results agree well with each other and confirm that the change from an axisymmetric to a three-dimensional geometry has not significantly affected the simulation. Both sets of results show good agreement with data, again matching to within a factor of 2-3 across the domain. Similar comparisons were made at different pressures to validate the 3D code, and all show the same level of agreement.

Once the code was validated, an effort was made to study the effect the plume of an SPT-100 would have on a realistic satellite configuration. Simulations were conducted on a simple GEO comsat as shown in Figure 1. The configuration consists of a bus, yoke, and solar array which are located on a 3.2 m x 4.4 m x 3.2 m domain. The dimensions of the spacecraft were discussed earlier. The spacecraft was assumed to be oriented with the arrays on the North and South sides of the spacecraft, so thrusters operating for N-S stationkeeping would fire in a vertical direction. The SPT-100 thruster was assumed to be mounted at the edge of the bus under the edge of the solar array as shown in Figure 1. The thruster's orientation was then varied during the simulations based on two parameters: a cant angle and an array angle. These angles are defined as shown in Figure 3. The cant angle is the angle between the thrust vector and the vertical axis. Lower cant angles better orient the thrusters for N-S stationkeeping, so higher cant angles represent an effective loss of I_{sp}. The array angle is defined as the solar panel's angle relative to an imaginary line connecting the yoke to the thruster. On a real spacecraft, the position of the thruster is fixed and the array turns with respect to the thruster. In our model, the array can only be turned in 90 degree increments. Therefore, to simulate different array angles, the thruster was mounted at different positions on top of the bus. This allows one to simulate a rotating array and still create a grid-conforming body. All simulations were run for 15000 time steps with a time step of 0.1 normalized units. The potential of the entire surface of the array was fixed at -92 volts relative to the center of the plume. A real array would be covered by cells with potentials that vary from 0 to 92 Volts. Setting the entire surface to -92 V therefore represents a worst case in which all parts of the array are assumed to sit at a very negative potential with respect to the spacecraft.

A cant angle of 45 degrees and an array angle of 45 degrees were chosen as the spacecraft's baseline configuration. Figure 4 shows the baseline configuration overlaid by a surface of constant potential. The plume is clearly visible as a cone emerging from the top of the bus and oriented away from the solar array. A contour plot of ion current density on the face of the array nearest to the plume shows a small but noticeable flux of ions reaching the surface even though the thruster is oriented away from the array. As one would expect, the area of highest flux is in the corner of the array which sits closest to the anode exit. Very little current reaches the lower or upper left corners of the array. Ions with relatively high energies are actually striking the upper right corner of the array, while ions with relatively low energy strike the corner nearest to the thruster. This occurs because high energy ions follow relatively straight trajectories and do not turn far enough to strike the lower part of the array. CEX ions, on the other hand, have a small turning radius and are easily influenced by electric fields at the edge of the plume. These ions turn quite sharply and end up striking the bottom of the array.

Figure 5 shows the calculated erosion rates for a silver surface of the array. The material is assumed to sit at -92 volts with respect to the center of the plume. This figure shows that a noticeable and potentially significant amount of erosion will occur to interconnectors on the solar array. As one would expect, the highest erosion rates occur on surfaces closest to the thruster. Silver's erosion rate is greater than 1 micron per month in some parts of the array. The actual area over which this high rate occurs is relatively small, covering an area of no more than 0.25 m^2. In addition, it should be noted that the surface is being held at a negative potential with respect to the plume. One obvious way to lower the peak erosion rate is to bias cells at the corners of the array positive with respect to the spacecraft. This would lower the energy of ions striking the surface of the array and help mitigate sputtering losses.

Canting the thruster away from the satellite's N-S axis lowers the thruster's effective I_{sp}, so it is desirable to use as small a cant angle as practical. To investigate the effects of changing the cant angle, simulations were run with cant angles from 0 to 45 degrees. Results suggest that a 15 degree change of angle has a significant impact on the erosion rates on the array. Not only is the peak sputtering rate more than 3 times higher than in Figure 5, but the area over which damage occurs extends much farther up the side of the array. A plume shield would almost certainly be required to limit damage to the array.

The relationship of most interest to spacecraft designers is the relationship between the cant angle, array angle, and the erosion rates experienced on the array. A series of simulations were conducted at different cant and array angles used to produce a map of the relationship between the array angle, cant angle, and erosion rates on the array.

Results from 21 runs were extrapolated to other cant and array angles using weighted averages based on one-over-distance-squared weighting factors. The results are summarized in Figure 6. This figure shows the erosion rate experienced at a point 20 cm from the bottom of the array and 20 cm from the side of the array, or about 30 cm away from the lower right corner. The upper left corners of the figure is significantly undersampled, but the cant and array angles in this quadrant are not generally of interest to spacecraft designers. As one would expect, lower cant and array angles result in higher erosion rates. The erosion rate varies by more than 2 orders of magnitude over the parameter space. From the plot, it is clear that silver interconnectors will undergo some erosion over the lifetime of the satellite. The allowable cant and array angles for this configuration depend on the acceptable erosion rate and the amount of time the array will be exposed to the plume from the SPT thrusters. Determining these rates requires knowledge of the thruster configuration and duty cycle. As a baseline case, it is assumed that the thruster is used for N-S stationkeeping with a 2000 kg. satellite in GEO over a lifetime of 12 years. The total Δv required is about 617 m/s.[15] It is also assumed that four thrusters are mounted on the satellite, two on the North and South faces respectively. Each SPT-100 thruster produces 85 mN of thrust, but because the four thrusters are canted with respect to the array, the effective thrust is less than this value. An effective thrust of 60 mN was assumed for this analysis. The total thruster operation time is given by

$$t = \frac{m\Delta v}{F}.$$

In this case, the resulting operation time is 2852 hours (4.0 months) over a twelve year satellite lifetime. The solar array orientation changes continuously as the satellite travels around the Earth. Only one side of the array produces power, and since erosion rates are very small at array angles greater than 90°, each half of the array is exposed to the plume from an SPT thruster only half of the time. This gives an effective exposure time of 1426 hours (2 months).

A typical solar cell interconnector is made of silver and is about 25 microns thick. When the interconnector erodes, the resistance in the connection increases and causes a power loss in the array. In this case, it was assumed that losses become significant when 10% of the interconnector's thickness has eroded away. This results in an allowable erosion depth of 2.5 microns which translates to an average rate of 1.2 microns/month over the lifetime of the satellite. Figure 6 shows the cant and array angles at which such rates can be achieved on the simulated spacecraft configuration. Even at a cant angle of 45 degrees, array angles greater than about 60° are required to avoid unacceptable erosion rates for the interconnectors. It should be noted that at high cant angles, only a small portion of the array is affected by the plume region. A mean rate of 1.2 microns/month can be achieved on this part of the array at cant angles of 35 degrees or less with the proper duty cycle. Installation of a plume shield might allow the use of even lower cant angles. Modeling the plume in the presence of a plume shield is within the capability of the present simulation but has not yet been completed. Modeling with plume shields is planned for future work.

Based on Figure 6, we conclude that cant angles greater than 40 degrees and array angles greater than 50 degrees are acceptable for the satellite considered in this study. These results only consider the effects of the plume on array interconnectors and depends on several important assumptions. First, the simulated array is biased at -92 V with respect to the thruster. Portions of the array biased at positive voltages will experience lower erosion rates. In addition, the interconnectors themselves sit between cells and may be partially shielded from the plume. On the other hand, the relatively small amounts of erosion which occur at array angles greater than 90 degrees have been neglected and non-normal ion impact angles are not included in the present model. These factors must all be considered when applying the simulation to real satellite configurations. Overall, interconnector erosion does not seem to be a fundamental barrier to the use of Hall Thrusters on satellites. However, we conclude that SPT thrusters will have to be canted with respect to the array, resulting in a lower effective specific impulse than the nominal value of 1600 seconds.

Conclusions

A computational model of an SPT plasma plume has been constructed using a quasi-neutral PIC-DSMC model. This model is based on theoretical work showing that the plume consists of a quasi-neutral plasma with collisionless electrons in which the magnetic field can be neglected. The resulting simulation can accurately model an SPT-100 plume on meter-length scales. Both axisymmetric and three-dimensional models have been developed and validated against experimental data. The results shown in this paper simulate conditions which can not be studied in ground-based experiments, including three-dimensional simulations of a SPT thruster mounted on a communications satellite. A series of three-dimensional simulations were conducted to demonstrate the model's ability to evaluate realistic spacecraft configurations. The results show that the thruster's cant angle has a strong impact on simulated erosion rates and the area over which erosion occurs. More importantly, the results demonstrate that the three-dimensional model can be adapted and used by spacecraft designers to evaluate realistic spacecraft configurations. This will help designers to quickly evaluate the impact of Hall Thrusters on a given spacecraft design.

Acknowledgments

The authors wish to thank David Manzella at NYMS Inc. for providing data used in this paper and Tom Randolph at SS/Loral for his help constructing a realistic satellite geometry. This paper was funded by the Air Force Office of Scientific Research.

References

[1]Manzella, D.H. "Stationary Plasma Thruster Plume Emissions," IEPC Paper 93-097, September 1993.

[2]Arkhipov, B.A. and Kozubsky, K.N. "The Development of the Cathodes-Compensators for Stationary Plasma Thrusters in USSR," IEPC Paper 91-023, October 1991.

[3]Myers, R.M. and Manzella, D.H. "Stationary Plasma Thruster Plume Characteristics," IEPC Paper 93-096, September 1993.

[4]Manzella, D.H. and Sankovic, J.M. "Hall Thruster Ion Beam Characterization," AIAA Paper 95-2927, July 1995.

[5]Rhee, M.S. and Lewis, M.J. "Numerical Simulation of Stationary Plasma Thruster Exhaust Plume," AIAA Paper 95-2928, July 1995.

[6]Dickens, J., Kirstiansen, M. and O'Hair, E. "Plume Model of Hall Effect Plasma Thrusters with Temporal Consideration," IEPC Paper 95-171, September 1995.

[7]Oh, D. and Hastings, D. "Axisymmetric PIC-DSMC Simulations of SPT Plumes," IEPC Paper 95-160, September 1995.

[8]Oh, D. and Hastings, D. "Experimental Verification of a PIC-DSMC Model for Hall Thruster Plumes," AIAA Paper 96-3196, June 1996.

[9]Randolph, T., Pencil, E. and Manzella, D. "Far-Field Plume Contamination and Sputtering of the Stationary Plasma Thruster," AIAA Paper 94-2855.

[10]Wang, Joe. "Electrodynamic Interactions Between Charged Space Systems and the Ionospheric Plasma Environment," Ph.D. Thesis, MIT Department of Aeronautics and Astronautics, June 1995.

[11]Rosenberg, D. and Wehner, G.K. "Sputtering Yields for Low Energy He+-Kr+-, and Xe+-Ion Bombardment," Journal of Applied Physics, Vol. 33, No. 5, May 1962, pp. 1842-1845.

[12]Chapman, B. *Glow Discharge Processes,* Wiley, New York, 1980, pg. 247.

[13]Qarnain, S. and Hastings, D.E. "Complete Computational Model of a Hall Thruster from the Acceleration Chamber through the Plume," IEPC 97-133.

[14]Oh, D.Y. and Hastings, D. "Three Dimensional PIC-DSMC Simulations of Hall Thruster Plumes and Analysis for Realistic Spacecraft Configurations," AIAA Paper 96-3299, June 1996.

[15]Larson, W.J. and Wertz, J.R. *Space Mission Analysis and Design*, 2nd ed., Microcosm, Torrance, CA, 1992, p. 151.

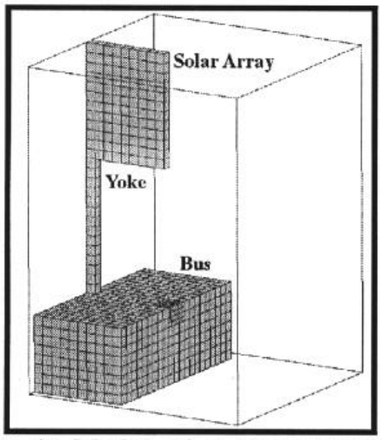

Figure 1: Model of a Communications Satellite on a 3D Embedded Mesh

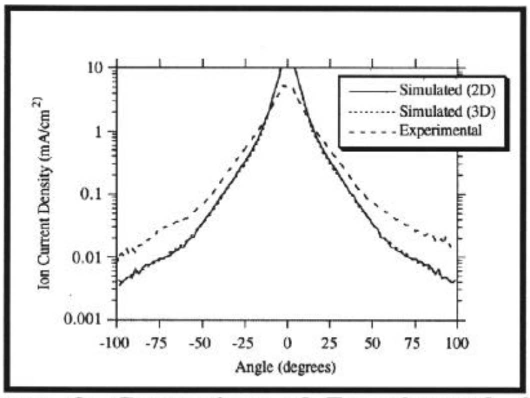

Figure 2: Comparison of Experimental, 2D, and 3D Simulations of Ion Current Density (z = 60 cm, $P = 2.2 \times 10^{-6}$ Torr)

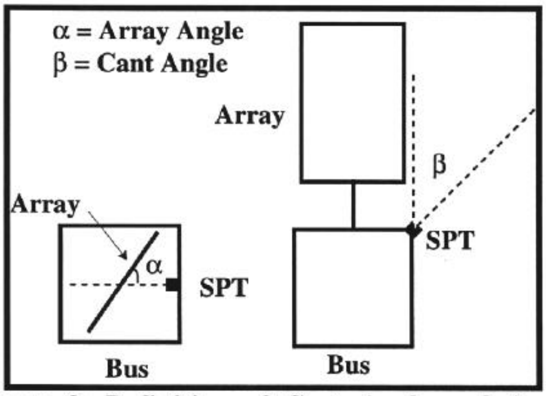

Figure 3: Definition of Cant Angle and Array Angle

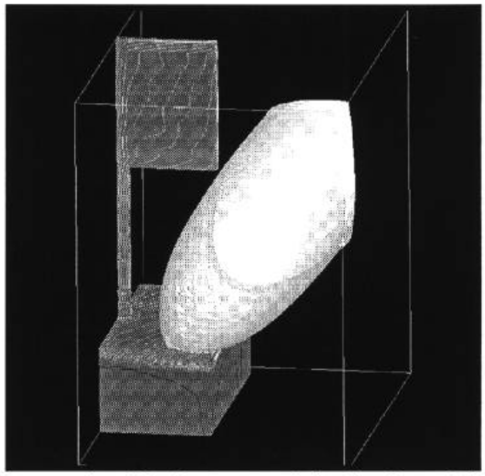

Figure 4: 3D Isopotential Surface Plot (Array Angle = 45°, Cant Angle = 45°)

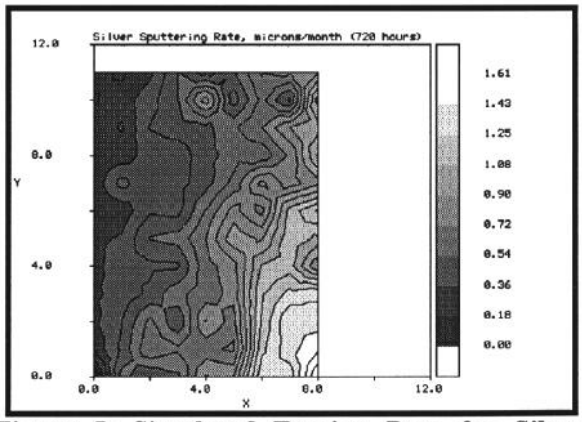

Figure 5: Simulated Erosion Rate for Silver (Array Angle = 45°, Cant Angle = 45°)

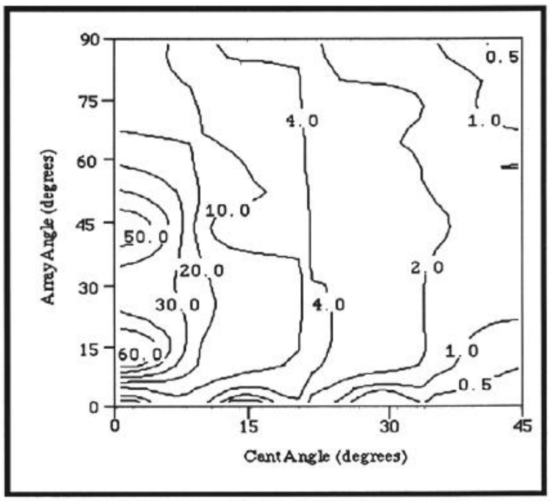

Figure 6: Erosion Rate [microns per month] for Silver 0.3 m from Corner of Array